Gene therapy for overexpressing Neuregulin 1 type I in skeletal muscles promotes functional improvement in the SOD1^{G93A} ALS mice

Guillem Mòdol-Caballero[a,b,1], Mireia Herrando-Grabulosa[a,b,1], Belén García-Lareu[b,c], Neus Solanes[a,b], Sergi Verdés[c], Rosario Osta[b,d], Isaac Francos-Quijorna[a,b,2], Rubèn López-Vales[a,b], Ana Cristina Calvo[b,d], Assumpció Bosch[b,c,e,*], Xavier Navarro[a,b,**]

[a] Department of Cell Biology, Physiology and Immunology, Institute of Neurosciences, Universitat Autonoma de Barcelona, Bellaterra, Spain
[b] Centro de Investigación Biomédica en Red sobre Enfermedades Neurodegenerativas (CIBERNED), Bellaterra, Spain
[c] Department of Biochemistry and Molecular Biology, Institute of Neurosciences, Universitat Autònoma de Barcelona, Bellaterra, Spain
[d] Laboratory of Genetics and Biochemistry (LAGENBIO), Faculty of Veterinary-IIS, University of Zaragoza, Zaragoza, Spain
[e] Vall d'Hebron Research Institute (VHIR), Barcelona, Spain

ABSTRACT

Amyotrophic lateral sclerosis (ALS) is a neurodegenerative disorder affecting motoneurons (MNs), with no effective treatment currently available. The molecular mechanisms that are involved in MN death are complex and not fully understood, with partial contributions of surrounding glial cells and skeletal muscle to the disease. Neuregulin 1 (NRG1) is a trophic factor highly expressed in MNs and neuromuscular junctions. Recent studies have suggested a crucial role of the isoform I (NRG1-I) in the collateral reinnervation process in skeletal muscle, and NRG1-III in the preservation of MNs in the spinal cord, opening a window for developing novel therapies for neuromuscular diseases like ALS. In this study, we overexpressed NRG1-I widely in the skeletal muscles of the SOD1^{G93A} transgenic mouse. The results show that NRG1 gene therapy activated the survival pathways in muscle and spinal cord, increasing the number of surviving MNs and neuromuscular junctions and reducing the astroglial reactivity in the spinal cord of the treated SOD1^{G93A} mice. Furthermore, NRG1-I overexpression preserved motor function and delayed the onset of clinical disease. In summary, our data indicates that NRG1 plays an important role on MN survival and muscle innervation in ALS, and that viral-mediated overexpression of NRG1 isoforms may be considered as a promising approach for ALS treatment.

1. Introduction

Amyotrophic lateral sclerosis (ALS) is a neurodegenerative disease characterized by loss of motoneurons (MNs) of primary motor cortex, brainstem and spinal cord (Wijesekera and Leigh, 2009). The vast majority of the cases are sporadic (sALS) in which the etiology is unknown, and about 10% correspond to familiar forms (fALS), associated with inherited alterations in genes, such as superoxide dismutase 1 (SOD1) (Rosen et al., 1993), TAR-DNA binding protein (TDP-43) (Kabashi et al., 2008; Yokoseki et al., 2008), hexanucleotide repeat expansions in chromosome 9 open reading frame 72 (C9orf72) (De Jesus-Hernandez et al., 2011; Renton et al., 2011), and others less

frequent. In both sALS and fALS the loss of MNs leads to rapid progressive muscle atrophy and weakness, accompanied with fasciculations and spasticity (Robberecht and Philips, 2013). The pathophysiological mechanisms underlying the development of ALS are multifactorial, with rising evidence of a complex interaction between genetic and molecular pathways (Mancuso and Navarro, 2015). The particular molecular mechanisms that specifically affect the MN to cause its death are still to be elucidated. Moreover, neighboring cells, such as microglia, astrocytes and interneurons, may contribute to the disease (Brites and Vaz, 2014). On the other hand, MN degeneration is preceded by alterations and disjunction of neuromuscular junctions (NMJs) (Fischer et al., 2004; Mancuso et al., 2011), and a toxic role for

skeletal muscle has also been reported (Moloney et al., 2014).

During the last decades several animal models carrying ALS-related mutations have been developed. The most widely used ALS model is a transgenic mouse expressing the human mutated form of the SOD1 gene with a glycine to alanine conversion at the 93rd amino acid (SOD1^{G93A}) (Gurney et al., 1994; Ripps et al., 1995), which outlines the most important clinical and pathological features of ALS in a rapid and severe progression of the disease (Ripps et al., 1995; Mancuso et al., 2011). Alterations in SOD1 protein have been also found in sporadic ALS patients (Bosco and Landers, 2010), and accumulation of wild-type SOD1 was shown to produce ALS in mice (Graffmo et al., 2013), thus, increasing the potential interest of the SOD1-linked ALS models.

Unfortunately, there is no cure for ALS, with only two drugs approved for use in ALS patients, riluzole, that slightly prolongs survival for 3–4 months, and edaravone, a drug that presumably works to mitigate oxidative injury in central neurons. Symptomatic and palliative measures (including feeding and respiratory support) are the mainstay of patients' management (Pasinelli and Brown, 2006). Recently, gene therapy for ALS has emerged as an alternative therapeutic strategy. The main advantage of this approach is that, by one single administration, it allows continuous expression of the therapeutic gene in specific tissues (Federici and Boulis, 2006). Among the different viral vectors, adeno-associated vectors (AAV) have some advantages over other viral vectors, such as the ability to provide sustained gene expression in terminally differentiated cells, avoiding the risk for insertional mutagenesis. Viral transgene expression can also be restricted depending on the viral tropism and using promoters with selective and defined expression patterns (Kügler, 2016).

Neurotrophic factors derived from the spliced forms of Neuregulin 1 (NRG1) have been shown to be critical for MN survival, supporting axonal and neuromuscular development and maintenance (Syroid et al., 1996; Sandrock Jr et al., 1997; Loeb et al., 1999; Wolpowitz et al., 2000; Nave and Salzer, 2006). NRG1 has been localized in spinal MNs, concentrated in the subsurface cisterns underlying postsynaptic sites of cholinergic C boutons (Issa et al., 2010; Gallart-Palau et al., 2014). NRG1 acts through the EGF domain of ErbB receptors, and NRG1-ErbB system alterations have been related to ALS, since loss-of-function mutations of ErbB4 produce late-onset, autosomal-dominant ALS in human patients (Takahashi et al., 2013). We have recently reported that ErbB4 ectodomain fragments were reduced in cerebrospinal fluid and plasma of ALS patients, suggesting impaired NRG1-ErbB signaling (Lopez-Font et al., 2019). Interestingly, several studies support that NRG1 type III expression is reduced in the spinal cord of both ALS patients and SOD1^{G93A} mice, whereas NRG1 type I appears to be up-regulated (Song et al., 2012; Mòdol-Caballero et al., 2019). Furthermore, viral-mediated delivery of NRG1-III in the spinal cord parenchyma restored the number of C-boutons and produced an increase of survival of the SOD1^{G93A} mouse (Lasiene et al., 2016). Also, intrathecal administration of an AAV coding for NRG1-III improves the progressive decline in motor function and MN number and reduces glial reactivity in SOD1^{G93A} mice (Mòdol-Caballero et al., 2019). However, the exact role of NRG1-I is not fully known. It has been reported that NRG1-I expression by Schwann cells is essential for promoting axonal regeneration and remyelination (Stassart et al., 2013). Indeed, overexpression of NRG1-I by means of an AAV vector, locally injected in the gastrocnemius muscle produced functional improvement by enhancing motor axons collateral sprouting in SOD1^{G93A} mice (Mancuso et al., 2016). Therefore, NRG-I plays a crucial role in the collateral re-innervation process. Considering these recent findings, our aim here was to overexpress NRG1-I in all the skeletal muscles using gene therapy vectors to maintain motor innervation in the SOD1^{G93A} mouse. For this reason, we administered intravenously AAV vectors under the regulation of the human desmin promoter, in order to restrict NRG1-I expression in skeletal and cardiac muscles.

2. Materials and methods

2.1. Animals

Transgenic mice carrying the mutation G93A in the SOD1 gene and non-transgenic wild-type (WT) littermates as controls were used. SOD1^{G93A} high copy mice (Tg[SOD1-G93A]1Gur) were obtained from the Jackson Laboratory (Bar Harbor, ME). These mice were bred and maintained as hemizygotes by mating transgenic males with F1 hybrid females obtained from Janvier Laboratories (France). Transgenic mice were identified by polymerase chain reaction amplification of DNA extracted from the tail. Mice were maintained in standard conditions with access to food and water ad libitum at the Animal Service of the Universitat Autònoma de Barcelona and were cared for and handled in accordance with the guidelines of the European Union Council (Directive 2010/63/EU) and Spanish regulations on the use of laboratory animals. The experimental procedures had been approved by the Ethics Committee of the Universitat Autònoma de Barcelona.

Sex-balanced therapeutic studies were performed using mice with B6xSJL background. The animals were divided in a group of WT mice and two groups of SOD1^{G93A} mice, that were administered at 6 weeks of age with either AAV8 coding for NRG1-I or mock vector. For the functional studies we used the following number of mice per group: WT mice ($n = 6$ females, $n = 5$ males), SOD Mock mice ($n = 14$ females, $n = 12$ males), SOD NRG1-I mice (n = 12 females, n = 5 males). These animals were then further distributed in two different subgroups at 16 weeks. One subgroup to analyze mRNA expression: WT ($n = 3$ females), SOD Mock ($n = 4$ females), SOD NRG1-I (n = 4 females); the second subgroup for histological analysis: WT (n = 3 females), SOD Mock (n = 4 females), SOD NRG1-I ($n = 7$ females).

2.2. Virus production and administration

The cDNA of the extracellular domain of NRG1-I isoform (provided by G. Corfas, Harvard Medical School, Boston, MA, USA) was cloned between AAV2 ITRs under the regulation of the human desmin promoter (provided by G. Lemke, Salk Institute, La Jolla, CA, USA). The woodchuck hepatitis virus responsive element (WPRE) was added at 3′ to stabilize mRNA expression. AAV2/8 stocks were produced by the Viral Production Unit of UAB-VHIR (http://viralvector.eu). Briefly, vectors were generated using the triple transfection system in HEK293-AAV cells of the expression plasmids, Rep2Cap8 plasmid containing AAV genes (provided by J.M. Wilson, University of Pennsylvania, Philadelphia, USA) and pXX6 plasmid containing adenoviral genes, needed as helper virus (Zolotukhin et al., 1999). After 48 h, AAV vectors were harvested, treated with benzonase, purified in an iodixanol gradient, and titred using the Picogreen (Invitrogen) system quantification (Piedra et al., 2015) and calculated as viral genomes per milliliter (vg/ml). AAV2/8 vectors containing the same regulatory sequences without the therapeutic gene (empty or mock vector) were used as control. A suspension of 7.6×10^{13} vg of AAV2/8 vectors in 250 μl was injected intravenously in 6 weeks- old mice via tail vein.

2.3. Electrophysiological tests

Motor nerve conduction tests were performed by stimulation of the sciatic nerve with single pulses of 20 μs duration (Grass S88) delivered by two needle electrodes placed at the sciatic notch. The compound muscle action potential (CMAP) was recorded from tibialis anterior (TA), gastrocnemius (GM) and plantar interossei (PL) muscles with microneedle electrodes (Mancuso et al., 2011) at 9, 12, 14 and 16 weeks of age. The recorded potentials were amplified and displayed on a digital oscilloscope (Tektronix 450S), measuring the latency and amplitude of the CMAP. The mouse body temperature was maintained constant by means of a thermostated heating pad.

Motor unit number estimation (MUNE) was performed using the

incremental technique (Mancuso et al., 2011) with the same setting as for motor nerve conduction tests. The sciatic nerve was stimulated with pulses of gradual increasing intensity, starting from a subthreshold intensity. Then, quantal increases in the CMAP were recorded. The increments higher than 50 μV were considered as due to the recruitment of an additional motor unit. The mean amplitude of single motor units was calculated as the average of consistent increases. The MUNE was calculated as the ratio between the CMAP maximal amplitude and the mean amplitude of single motor unit action potentials.

To evaluate the central descending pathways, motor evoked potentials (MEP) were recorded from TA and GM muscles following electrical stimulation of the motor cortex with pulses of 0.1 ms duration and supramaximal intensity, delivered with needle electrodes placed subcutaneously over the skull overlaying the sensorimotor cortex (Mancuso et al., 2011).

2.4. Locomotion tests

The Rotarod test was performed to evaluate motor coordination, strength and balance of the animals. Mice were placed onto the rod rotating at a constant speed of 14 rpm. The time that the animal remained on the rotating rod was measured. Each mouse was given three trials and the longest time until falling recorded; 180 s was chosen as the arbitrary cut-off time. The test was performed from 9 to 16 weeks of age. Clinical disease onset for each mouse was determined as the first week when the maintenance time was lower than 180 s.

2.5. RNA extraction and real time PCR

To obtain DNA or RNA samples, mice were sacrificed at 16 weeks of age by decapitation after deep anesthesia. Gastrocnemius muscle and L4-L5 spinal cord segments were rapidly dissected. DNA was extracted from spinal cord with 0.1 mg/ml of proteinase K (Roche Diagnostics), followed by phenol/chloroform extraction. Real time primers for cyclophilin B, as housekeeping gene, or Desmin-NRG1.1 construct, where the forward primer is located in the desmin promoter sequence and the reverse primer in the Nrg1.1 cDNA sequence, are listed in Supplementary Table 1. Viral genome copies per cell were calculated using a standard curve generated from known amounts of a plasmid DNA containing the Desmin-NRG1.1 sequence or a 525 bp cyclophilin PCR product purified by Geneclean (Q-Biogene) in 10 ng per ml of salmon's sperm DNA (Sigma) and assuming that 1 mg of mouse genomic DNA contains 3×10^5 haploid genomes.

For mRNA analyses, tissues were homogenized in Qiazol (Qiagen) using a Tissue Lyser LT (Qiagen) at 50 Hz twice. One μg of RNA was reverse-transcribed using 10 μmol/l DTT, 200 U M-MuLV reverse transcriptase (New England BioLabs), 10 U RNase Out Ribonuclease Inhibitor (Invitrogen), 1 μmol/l oligo(dT), and 1 μmol/l of random hexamers (New England BioLabs). The reverse transcription cycle conditions were 25 °C for 10 min, 42 °C for 1 h and 72 °C for 10 min. We analyzed the mRNA expression of Nrg1.1, ErbB2, ErbB3 and ErbB4, by means of specific primer sets (Supplementary Table 1). Mouse 36B4 was used to normalize the expression levels of the different genes of interest for mouse samples. Gene-specific mRNA analysis was performed by SYBR-green real-time PCR using the MyiQ5 real-time PCR detection system (Bio-Rad). The thermal cycling conditions comprised 5 min polymerase activation at 95 °C, 45 cycles of 15 s at 95 °C, 30s at 60 °C, 30s at 72 °C and 5 s at 65 °C to 95 °C (increasing 0.5 °C every 5 s). Fluorescence detection was performed at the end of the PCR extension, and melting curves were analyzed by monitoring the continuous decrease in fluorescence of the SYBR Green signal. Quantification relative to 36B4 controls for mRNA or Cyclophilin for DNA was calculated using the Pfaffl method (Pfaffl, 2001).

2.6. Western blot analysis

Fresh gastrocnemius muscle and lumbar spinal cord tissues were sonicated and homogenized in RIPA lysis buffer (50 mM Tris-Cl pH 7.4, 150 mM NaCl, 1 mM EDTA, 1% NP-40, 0.25% sodiumdeoxycholate) containing a mixture of protease inhibitors (Millipore). Protein concentration was determined by PierceTM BCA Protein Assay Kit (Thermo Scientific). Between 25 and 35 μg of protein were separated on 10% SDS-polyacrylamide gel electrophoresis gel (VWR Life Science), transferred to polyvinylidene difluoride membranes (GE Healthcare) and immunoblotted. The following antibodies were used: rabbit anti-phospho Akt (1:500, Ser473 #9271, Cell Signaling), total Akt (1:500; #9272 Cell Signaling), rabbit anti-phospho Erk1/2 (1:500, #9101 Thr202/Tyr204, Cell Signaling), total Erk (1:500; #9102, Cell Signaling), rabbit anti-GAPDH (1:1000; #14C10, Cell Signaling), and mouse anti-gamma tubulin T6557 (1:1000; Sigma-Aldrich). Detection was performed with swine anti-rabbit HRP-conjugated secondary antibody (1:10,000; Dako) and Westar Eta C Ultra 2.0 ECL substrate (CYANAGEN). Image LabTM software (Bio-Rad) was used for image density quantification. Minimum of 3 animals per group and treatment were used and at least 3 different blots were quantified for each marker.

2.7. Measurement of muscle biomarkers

The gene expression analysis was performed by real-time PCR (7500 Real-Time PCR System, Applied Biosystem, Madrid, Spain). Two target genes related to skeletal muscle homeostasis and regeneration were included in this analysis: Collagen type XIX alpha 1 (Col19a1), Myocyte enhancer factor 2C (Mef2c) and glutathione reductase (Gsr). The Taqman probes (Applied Biosystems, Madrid, Spain) (Col19a1: Mm00483576_m1; Mef2c: Mm00600423_m1; Gsr: Mm00833903_m1; see Supplementary Table 1) used in this study were tested and in all the cases the efficiency was near 100%. All the real-time PCR reactions were done in triplicate and two endogenous genes (beta actin, β-actin, 4352932E, and glyceraldehyde 3-phosphate dehydrogenase, Gapdh, 4352933E) were used to normalize the target gene expression. The ΔΔCt method was used to determine relative changes in transcriptional expression. Statistical analyses of the data were performed using the fold change $2^{-\Delta\Delta Ct}$.

2.8. Histological analysis

At 16 weeks of age, subgroups of mice were transcardially perfused with 4% paraformaldehyde in PBS, and the lumbar spinal cord and the gastrocnemius muscle were harvested. Spinal cords were post-fixed during 2 h, then cryopreserved in PBS with 30% sucrose. GM muscles were directly cryopreserved.

For spinal MN counting, cord samples were cut in 20 μm thick transverse sections and serially collected in gelatinized slides. For each animal, slides corresponding to L4-L5 spinal cord sections with a separation of 100 μm were stained with cresyl violet. MNs were identified by their localization in the ventral horn and strict size and morphological criteria (Mancuso et al., 2011).

For glial cell reactivity, L4-L5 spinal sections were blocked with PBS-0.3%Triton-10% Normal Donkey serum and 20 mM glycine, and incubated 24 h at 4 °C with primary antibodies anti-ionized calcium binding adapter molecule 1 (Iba-1, 1:1000; 019–19,741, Wako, Japan), and anti-glial fibrillary acidic protein (GFAP, 1:1000; 130,300, Invitrogen, USA) to label microglia and astroglia respectively. After washes, sections were incubated overnight with Alexa 488-conjugated secondary antibody (1:200; A21206, Invitrogen, USA) or Cy3-conjugated secondary antibody (1:200; 712–165-150, Jackson IR, USA). DAPI (1:2000; D9563-10MG, Sigma, USA) was used to stain cell nucleus. Slides were mounted in Fluoromount-G (Southern Biotech, USA) and viewed under a fluorescence microscope (Nikon Eclipse NI, Japan). A region of interest centered in the ventral horn was selected to

measure the integrated density of Iba1 and GFAP labeling using ImageJ software (NIH, Bethesda, MD).

For muscle immunohistochemistry, 60 μm longitudinal sections were serially cut and collected in 24-well plates in sequential series of 4 slices per well in Olmos solution. Sections were blocked with PBS-0.3%Triton-5%Normal Donkey serum and incubated 48 h at 4 °C with primary antibodies anti-synaptophysin (1:500; AB130436, Abcam, UK) and anti-neurofilament 200 (NF200, 1:1000; AB5539, Millipore, USA). After washes, sections were incubated overnight with Alexa 594-conjugated secondary antibody (1:200; A11042, Invitrogen, USA) and Alexa 488 conjugated alfa-bungarotoxin (1:200; B13422, Life Technologies, USA). Confocal images were captured with a scanning confocal microscope (LSM 700 Axio Observer, Carl Zeiss 40×/1.3 Oil DIC M27, Germany). Maximum projections images shown in this study were generated from 1.5 μm z projections. For NMJ analysis, the proportion of innervated endplates was calculated by classifying each endplate as fully occupied (when presynaptic terminals overlie the endplate), partially occupied (when presynaptic terminals were not clearly within the endplate) or vacant (no presynaptic label in contact with the endplate). At least 4 fields with more than 100 endplates were analyzed per muscle.

2.9. Statistical analysis

All experiments were performed by researchers blinded with respect to treatment received by each mouse group, and random allocation of animals in groups taking into account weight and litter. Data are expressed as mean ± SEM. Electrophysiological and locomotion tests results were statistically analyzed using one-way or repeated measurements ANOVA with Tukey's post-hoc test. For the MUNEs and MEPs electrophysiological results Student's t-test was applied. For clinical disease onset data Log-rank (Mantel-Cox) test was applied. Histological and molecular biology data were analyzed using ANOVA and t-Student.

3. Results

3.1. Viral-delivery of NRG-I in skeletal muscles

We first tested the transduction of the AAV8-desmin-NRG1-I vector in the skeletal muscles based on a single intravenous injection of 7.6×10^{13} vg in 250 μl in 6 weeks-old mice, in order to obtain a high expression of NRG1-I during the symptomatic stage, starting between 8 and 10 weeks of age in this model. At the end stage of the disease (16 weeks) we confirmed that the treated SOD1^{G93A} mice had a higher expression of NRG1-I in the GM muscle (18.64 ± 7.09 fold) compared to the SOD1^{G93A} mock mice (0.76 ± 0.41) (Fig. 1A). This result agreed with the detection of 0.24 ± 0.05 viral genomes of Desmin-NRG1.1/cell detected in the treated SOD1^{G93A} mice (Fig. 1B).

3.2. NRG1-I overexpression preserves neuromuscular function of the treated SOD1^{G93A} mice

To study the effect of the NRG1-I overexpression, we evaluated by means of electrophysiological tests the neuromuscular function in hindlimb muscles of SOD1^{G93A} mice. The results showed that there was a significant preservation of the PL, TA and GM CMAP amplitude at 16 weeks in the female (Fig. 2A,B,C) and male treated SOD1^{G93A} mice (Supplementary Fig. 1A,B,C) compared to the control mice. This higher CMAPs amplitude of hindlimb muscles was explained by an increase of the mean amplitude and the number of surviving motor units in female (Fig. 2D,E,F) and also male mice (Supplementary Fig. 1D,E,F). The distribution of TA motor units grouped by amplitude of the action potential show a higher number in most of the intervals for female (Fig. 2F) and male mice (Supplementary Fig. 1F). The amplitude of the MEPs recorded in the GM and TA muscles was also significantly higher in treated SOD1^{G93A} mice (Fig. 2G and Supplementary Fig. 1G).
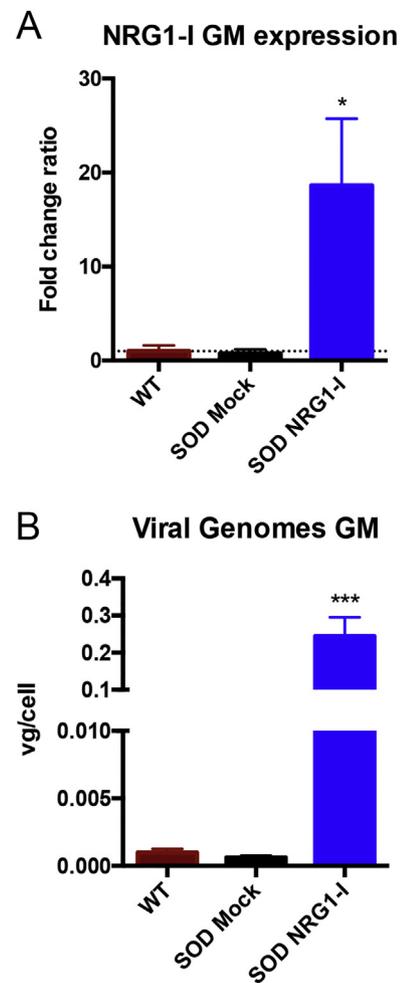

Fig. 1. *AAV8 under the desmin promoter coding for NRG1-I enhances NRG1-I expression in the hindlimb muscles of SOD1^{G93A} mice.* A) mRNA expression analysis shows that NRG1-I is overexpressed in the GM muscle of treated mice compared to the control SOD1^{G93A} and WT mice. B) Viral genome analysis reveals that intravenous AAV injection was effective in the treated mice. ($n = 5$ WT, 4 SOD Mock, 4 SOD NRG1-I mice per group, one-way ANOVA, ***$p < .001$, *$p < .05$ vs SOD Mock mice). Data are shown as mean ± SEM.

3.3. NRG1-I overexpression preserves spinal MNs and reduces neuroinflammation

We then performed the histological analysis of the SOD1^{G93A} mice at 16 weeks. The results showed that the NRG1-I overexpression in skeletal muscles preserved the number of MNs (12.1 ± 0.5 mean number of MNs per ventral horn ± SEM) compared to the SOD1^{G93A} mock mice (6.0 ± 0.5) (Fig. 3A,B) in line with our electrophysiological findings. The increased CMAP and motor unit number in the hindlimb muscles at 16 weeks was further confirmed by the NMJ analysis, since the NRG1-I gene therapy significantly preserved the number of occupied motor endplates (68.8 ± 5.1 percentage of occupied endplates ± SEM) compared to the mock SOD1^{G93A} group (35.9 ± 7.2) (Fig. 3A,B). We also assessed the glial immunoreactivity in the spinal cord and we found a significant decrease of astrocyte and microglial activation ($3.89 \times 10^7 ± 6.60 \times 10^6$ and $5.52 \times 10^7 ± 1.08 \times 10^7$ respectively; integrated density ± SEM) compared to the SOD1^{G93A} mock mice ($1.825 \times 10^8 ± 2.67 \times 10^7$ and $2.25 \times 10^8 ± 9.07 \times 10^7$ respectively) (Fig. 3C,D).
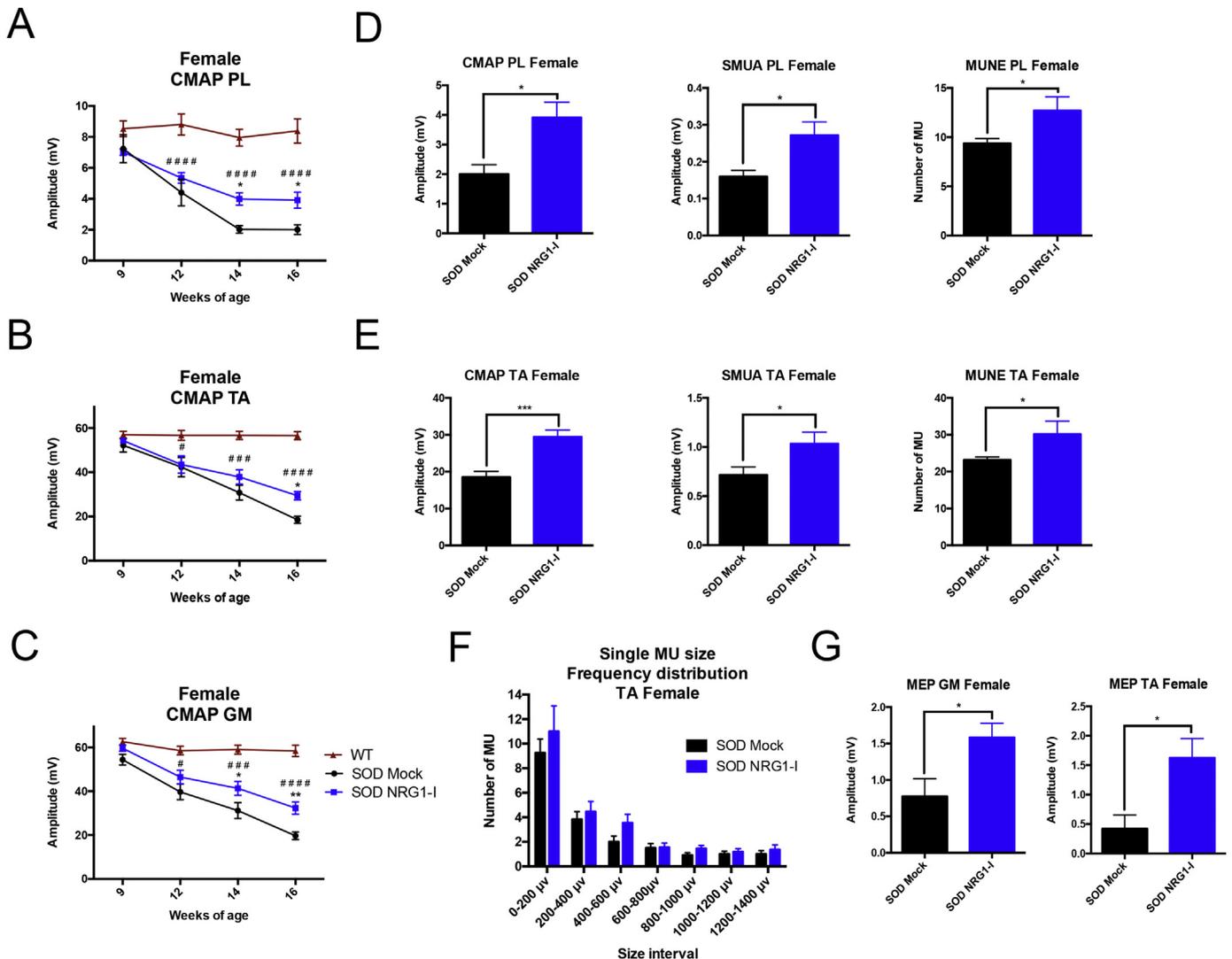
Fig. 2. *NRG1-I overexpression promotes motor functional improvement of the SOD1^G93A mice.* A) Electrophysiological tests show that AAV-NRG1-I injection produced a significant preservation of the CMAP amplitude of PL (A), TA (B), and GM (C) muscles in the SOD1^G93A mice along time (*n* = 6 WT, 6–13 SOD Mock, 10–11 SOD NRG1-I mice per group, two-way ANOVA, **p < .01, *p < .05 vs SOD Mock mice; ####*p* < .0001, ###*p* < .001, #*p* < .05 vs WT mice). Electrophysiological estimation of motor unit number (MUNE) and mean amplitude of single motor unit potential (SMUA) of the PL (D) and TA (E) muscles show that the increased CMAP amplitude was the result of preservation of more motor units and of larger size, confirmed by the frequency distribution (F). G) NRG1-I treatment increased the amplitude of the MEPs (n = 6–14 SOD Mock, 10–12 SOD NRG1-I mice per group, T-student, ***p < .001, *p < .05 vs SOD Mock mice). Data are mean ± SEM.

3.4. NRG1-I signaling through ErbB receptors produces motor functional improvement in the treated SOD1^G93A mice

We evaluated the expression of the ErbB 2, 3 and 4 receptors in GM muscle samples of SOD1^G93A mice. While no changes were detected between WT and mock-treated SOD mice for the ErbB receptors mRNA, upon NRG1-I overexpression, mRNA levels of ErbB2 (1.7 ± 0.42-fold increase compared to WT levels) (Fig. 4A) and ErbB3 (3.36 ± 0.26) (Fig. 4B) were significantly upregulated compared to SOD1^G93A mock and WT mice (0.59 ± 0.12 and 1.57 ± 0.43 respectively). The ErbB4 receptor levels were also increased in NRG1-I SOD1^G93A treated mice (1.48 ± 0.66) compared to the SOD1^G93A mock group (0.79 ± 0.13) but the differences were not statistically significant (Fig. 4C).

We also explored cell signaling pathways to corroborate functional activity of the Nrg1/ErbB axis by western blot analysis of GM muscle. We found that activation of Akt was strongly downregulated in SOD1^G93A mice and NRG1-I treatment completely restored Akt phosphorylation compared to the mock treated group (Fig. 4D). On the contrary, activation of Erk in SOD1 animals is high, particularly in the p42 isoform, in agreement with previous reports (Bhinge et al., 2017;

Mòdol-Caballero et al., 2019). Nrg1-I treatment significantly reduced the ratio of phosphorylation of Erk2 (Fig. 4D). We also evaluated activation of cell survival pathways in the spinal cord, where we found similar results than in muscle: NRG1-I overexpression in muscle activated Akt phosphorylation but decreased ERK activation, particularly of p42, returning to control levels (Fig. 4E).

In order to better characterize muscle homeostatic maintenance, we analyzed the expression of genes related to ALS disease progression in the muscle by quantitative real time PCR. Two target genes, *Col19a1* and *Mef2c*, were found increased in the GM muscle of SOD1^G93A mice, as previously reported (Calvo et al., 2012). Albeit no statistical significant difference was found between untreated SOD1^G93A mice and NRG1-I treated mice regarding *Col19a1* and *Mef2c* gene levels (Fig. 4F), probably due to the variability of the samples, NRG1-I treated mice showed a tendency to have lower *Col19a1* and *Mef2c* mean levels, suggesting that NRG1-I could ameliorate muscle damage during progressive denervation. In addition, we aimed to investigate if NRG1-I treatment was able to reduce oxidative stress in the muscles, as previously described in adult rat cardiomyocytes (Timolati et al., 2006). Therefore, we investigated the gene expression levels of glutathione
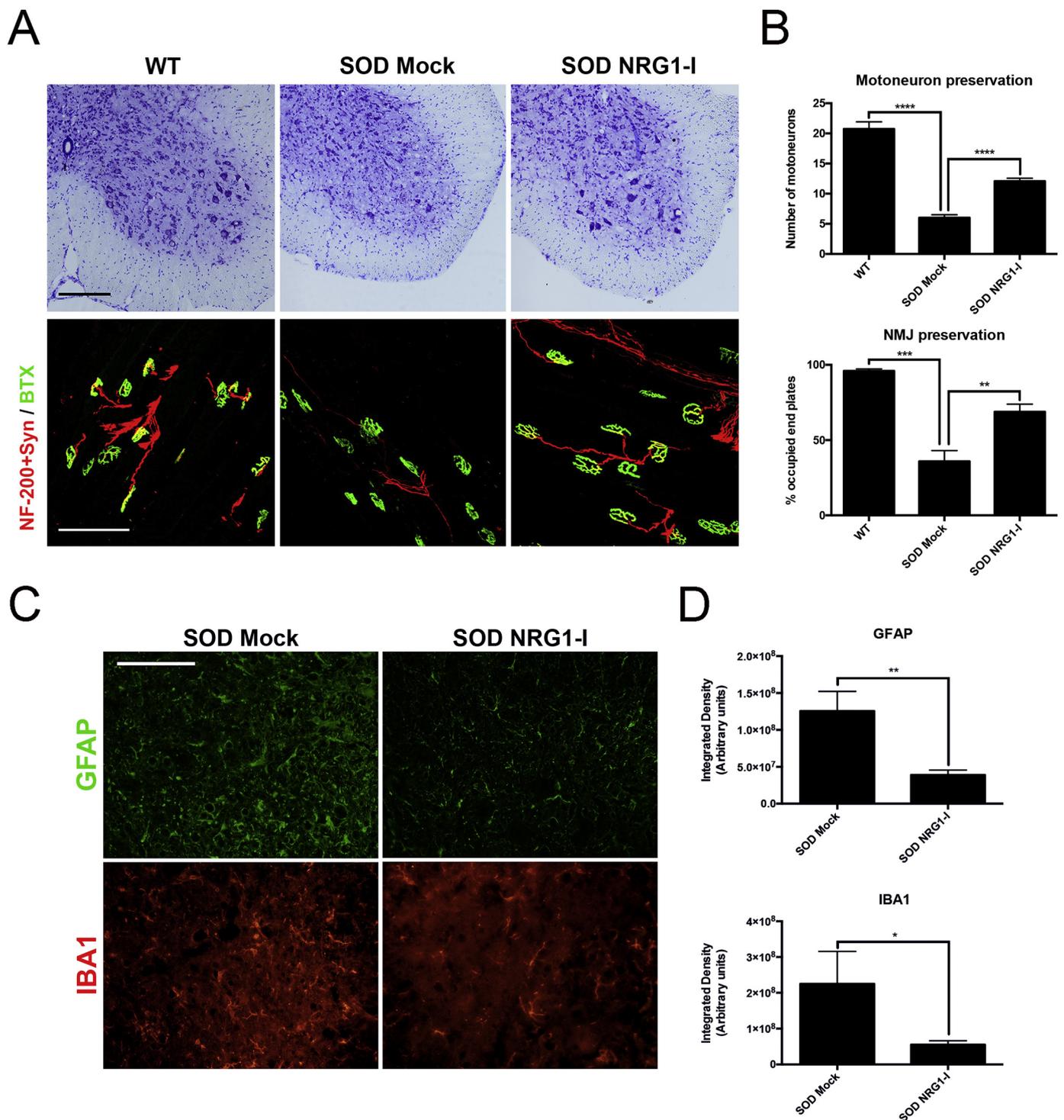
Fig. 3. *Viral-delivery of NRG1-I preserves spinal MN number and decreases glial reactivity.* A) Representative images of L4 spinal cord and GM neuromuscular junctions of WT and SOD1[G93A] mice, treated with AAV-NRG1-I or with mock vector (scale bar = 100 μm). B) Histological analysis showed higher number of spinal MNs, as well as increased proportion of innervated NMJs in the GM muscle in the treated SOD1[G93A] mice compared to the mock treated mice (n = 3 WT, 3–4 SOD Mock, 7 SOD NRG1-I mice per group, one-way ANOVA, ****p < .0001, ***p < .001, **p < .01 vs SOD Mock mice). C) Representative confocal images of astrocytes labeled against GFAP, and microglia labeled against Iba-1, in the spinal cord ventral horn of SOD1[G93A] mice (scale bar = 100 μm). D) The viral-mediated delivery of NRG1-I reduced the astrocyte and microglia reactivity in the treated SOD1[G93A] mice (n = 3–4 SOD Mock, 5–6 SOD NRG1-I mice per group, T-student, **p < .01, *p < .05). Data are shown as mean ± SEM.

reductase (*Gsr*), previously identified altered in SOD1[G93A] mice and closely related to the oxidative stress metabolism (Calvo et al., 2012). Interestingly, *Gsr* levels were found significantly decreased in NRG1-I treated mice compared to mock treated SOD1[G93A] mice (Fig. 4F), indicating that NRG1-I reduced oxidative stress in the GM muscle.

Altogether these data suggest a mechanism of protection from excitotoxicity and inflammation and activation of the cell survival pathways both in muscle and in spinal cord. Consequently, NRG1-I/ErbB signaling in the skeletal muscles was able to produce also functional improvement in the rotarod performance in the treated SOD1[G93A] mice
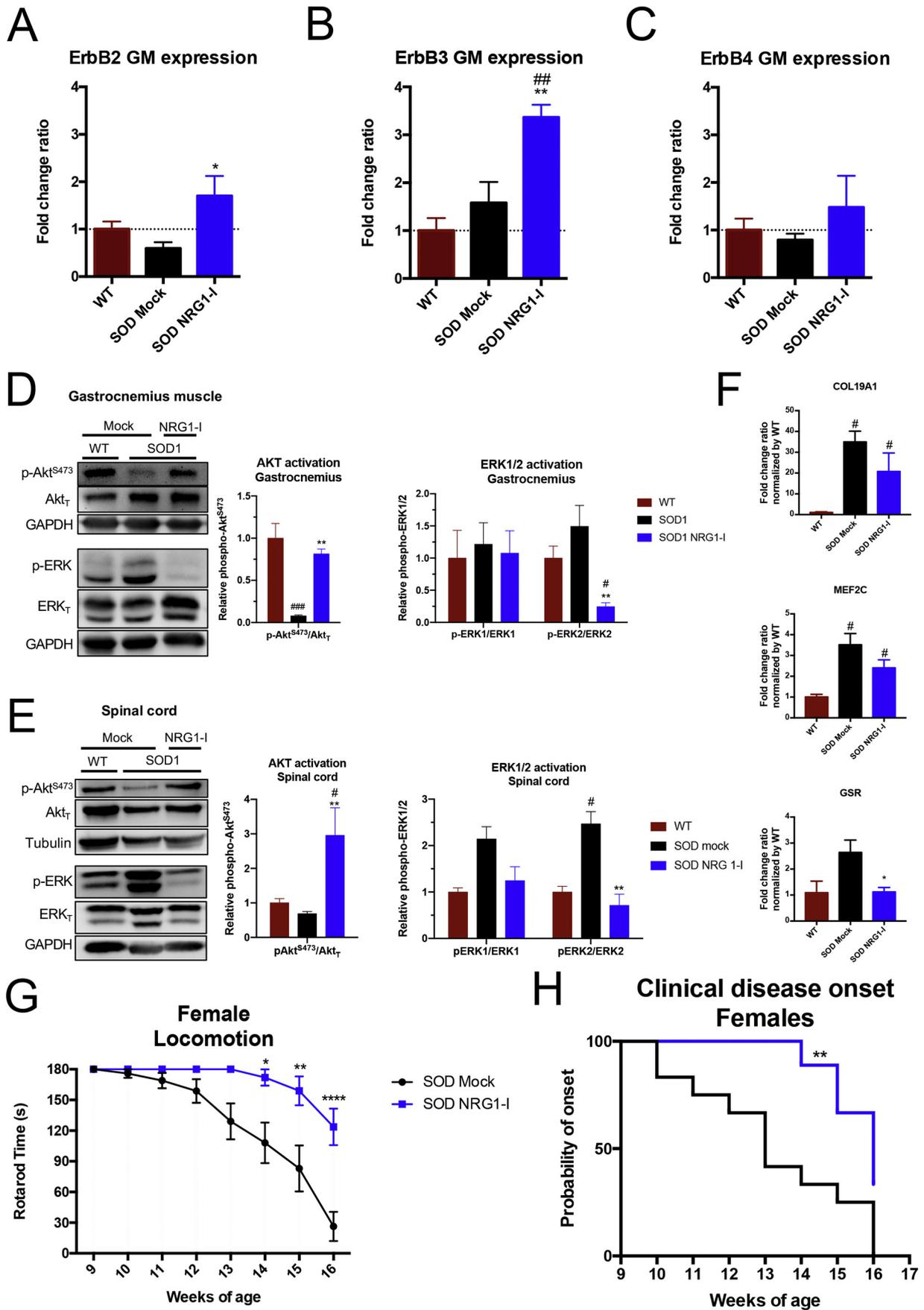
(caption on next page)

Fig. 4. *Increased NRG1-I/ErbB signaling activates survival pathways in muscle and spinal cord and produces functional improvement in the treated mice.* mRNA expression analysis of ErbB receptors shows a significant upregulation of ErbB2 (A) and ErbB3 (B) upon NRG1-I overexpression in the treated SOD1^{G93A} mice compared to the mock mice, whereas the levels of ErbB4 receptor (C) showed a non-significant increase (n = 3 WT, 3–4 SOD Mock, 4 SOD NRG1-I mice, one-way ANOVA, **p < .01, *p < .05 vs SOD Mock mice, ##p < .01 vs WT mice). D) NRG1-I increases Akt phosphorylation and diminishes Erk2 activation in the muscle of SOD1^{G93A} treated animals, as demonstrated by Western blot. E) Muscle NRG1-I increases Akt phosphorylation and normalizes ERK2 activity in the spinal cord of treated SOD1^{G93A} mice. Quantifications show relative phosphorylation compared to total protein, normalized by GAPDH and are represented by fold-change compared to WT animals; **p < .01 vs SOD Mock mice, ###p < .0005, #p < .05 vs WT mice). F) mRNA expression of muscle biomarkers *Col19a1*, *Mef2c* and *Gsr* (n = 3 for each group; #p < .05 vs WT mice and *p < .05 vs SOD Mock mice). G) NRG1-I overexpression produced an improvement in the rotarod performance of treated SOD1^{G93A} mice from 14 to 16 weeks (n = 12 SOD Mock, 7 SOD NRG1-I mice per group, two-way ANOVA, ****p < .0001, **p < .01, *p < .05 vs SOD Mock mice). Data are shown as mean ± SEM. H) Clinical onset of disease was significantly delayed (n = 12 SOD Mock, 9 SOD NRG1-I mice per group, Mantel-Cox test, **p < .01, vs SOD Mock mice).

(Fig. 4G) and a significant delay of the clinical disease onset (Fig. 4H) compared to the control SOD1^{G93A} mice.

4. Discussion

We previously showed that NRG1-I overexpression localized in the GM muscle produced functional compensation by enhancing collateral sprouting in the SOD1^{G93A} mouse and in WT mouse after partial muscle denervation (Mancuso et al., 2016). However, an increased expression of NRG1-I in a single muscle was only a proof of principle, since it was not able to globally improve ALS disease progression. Therefore, we attempted to promote a general overexpression of NRG1-I in most skeletal muscles to produce global functional improvement by intravenous administration of an AAV vector under the regulation of the desmin promoter. Indeed, NRG1-I acting through the ErbB receptors in the periphery causes neuromuscular functional improvement, maintains NMJ innervation and increases spinal MN survival in both female and male mice, while reducing glial cell reactivity around MNs in the SOD1^{G93A} mice that received a single administration of the viral vector.

NRG1 isoforms are important trophic factors that play multiple roles in the nervous system development and maintenance (Esper et al., 2006). Alterations of the NRG1/ErbB system have been related to ALS (Takahashi et al., 2013; Lopez-Font et al., 2019). NRG1-III expression was found reduced in the spinal cord of both ALS patients and SOD1^{G93A} mice in parallel with MN loss (Song et al., 2012; Lasiene et al., 2016; Mòdol-Caballero et al., 2019). Indeed, viral-mediated delivery of NRG1-III in the CNS restored the number of C-boutons and produced a slight increase of survival of the SOD1^{G93A} mice (Lasiene et al., 2016). We recently demonstrated that addition of NRG1 exerts neuroprotective effects on MNs under chronic excitotoxicity in an in vitro model (Mòdol-Caballero et al., 2018), and that overexpression of NRG1-III along the spinal cord of SOD1^{G93A} mice improves motor function and MNs survival (Mòdol-Caballero et al., 2019).

However, the role of NRG1-I isoform in MN degenerative diseases remains unclear. NRG1-I is critical for the axoglial intercommunication during development (Loeb et al., 1999; Esper and Loeb, 2004), the formation of muscle spindles (Andrechek et al., 2002; Hippenmeyer et al., 2002) and the maintenance of the mature NMJ (Sandrock Jr et al., 1997; Loeb et al., 2002; Loeb, 2003). Indeed, NRG1/ErbB signaling is important for the stability of acetylcholine receptors at the NMJ and the structural integrity of the postsynaptic site (Schmidt et al., 2011). While Song et al. (2012) found that NRG1-I isoform was increased and associated with glial activation in the spinal cord of SOD1^{G93A} mice in agreement with our recently published results (Mòdol-Caballero et al., 2019), Lasiene et al. (2016) showed decreased NRG1-I mRNA levels. However, when they applied a virus-mediated delivery to overexpress this isoform in the lumbar spinal cord parenchyma, their results were less beneficial than with NRG1-III (Lasiene et al., 2016).

In this study, we found that overexpression of NRG1-I in skeletal muscles produced an upregulation of the ErbB receptors, which in turn, are expressed by the terminal Schwann cells in the NMJs (Syroid et al., 1996). Indeed, bidirectional communication between Schwann cells and MNs supports their mutual survival and differentiation during

development and after nerve injury (Esper and Loeb, 2004). NRG1-I overexpression promotes axonal regeneration and remyelination in a transient autocrine/paracrine signaling loop with Schwann cells expressing ErbB2 and 3 receptors (Stassart et al., 2013). Moreover, constitutively active ErbB2 in Schwann cells resulted in proliferation and process extension from these cells (Hayworth et al., 2006), and loss of NRG1/ErbB signaling destabilizes the anchoring of acetylcholine receptors in the postsynaptic muscle membrane (Schmidt et al., 2011). Also, considering that only the extracellular domain of NRG1-I was overexpressed in our study, we cannot discard an intracrine signaling of NRG1-I by the muscle cells that could explain the NMJ maintenance (Wiley et al., 1998). Therefore, NRG1-I expressed at the NMJ may act on terminal Schwann cells and on muscle fibers, promoting maintenance of muscle innervation and motor axon survival. This is in accordance with the findings obtained in target biomarkers of muscle degeneration and oxidative stress. NRG1-I gene therapy promoted lower mean values of *Col19a1* and *Mef2c* mRNA with respect to untreated mice, although not significantly (Calvo et al., 2012). *Col19a1* is involved in the maintenance of muscle integrity, albeit it has been also described to play a role in differentiation of muscle cells, in a similar way to *Mef2c* gene. Structural or functional alterations of skeletal muscle in MN disease can alter the transmission of chemical and electrical signals between motor axons and NMJ, favoring the dying-back phenomenon and therefore contributing to disease pathology (Ferraiuolo et al., 2009). Interestingly, transcript levels of collagen type I and III were found reduced in the myocardium of a murine model of diabetic cardiomyopathy after NRG1 administration, promoting an improvement of cardiac function (Li et al., 2011). In this study, the tendency to lower *Col19a1* and *Mef2c* mean levels suggests an enhancement of muscle integrity and homeostasis. In addition, the significant reduction in Glutathione reductase (*Gsr*) levels in NRG1-I treated mice also suggests that NRG1-I treatment ameliorates oxidative stress in the skeletal muscle. Glutathione reductase maintains the supply of reduced glutathione, which is one of the most abundant reducing thiols in the majority of cells, modulating the reactive oxygen species (Couto et al., 2016). The reduction of *Gsr* levels in NRG1-I treated mice would indicate a better modulation of the redox homeostasis, that depends on ErbB2 and Akt receptors, as was described in rat cardiomyocytes (Timolati et al., 2006). Taking together these findings, NRG1-I appear to positively influence the response to muscle denervation and secondary damage.

Furthermore, NRG1-I therapy restored Akt phosphorylation in muscle and spinal cord of ALS mice. On the contrary, SOD1^{G93A} animals with B6xSJL background show activation of Erk1/2 as we previously described (Modol-Caballero et al., 2019), as well as do MNs derived from iPS cells from SOD1 ALS patients (Bhinge et al., 2017). NRG1-I treatment significantly reduced Erk activation, so the imbalance between Akt and Erk1/2 was restored. A similar imbalance was described in rodent models of CMT1A and soluble NRG1–1 overexpression restored such dysregulation and preserved peripheral nerve axons (Fledrich et al., 2014). Nevertheless, it has been reported that soluble NRG1-I overexpression may promote demyelination (Zanazzi et al., 2001; Syed et al., 2010; Fledrich et al., 2019). The adverse effect on demyelination is driven by the activation of Erk pathway, which was

found reduced when our NRG1-I therapy was applied. Moreover, our electrophysiology data showed that for both TA and PL muscles the CMAP latencies were similar in SOD untreated and treated groups (data not shown). The latency time reflects the conduction velocity and thus, shows if myelinated fibers are affected in ALS (Cornblath et al., 1992; de Carvalho and Swash, 2000) and in other diseases. Therefore, we can discard the potential side effect of demyelination induced by the NRG1-I overexpression therapy. Altogether these data suggest a mechanism of protection from excitotoxicity and inflammation, and activation of the cell survival pathways both in muscle and in spinal cord.

It is worth to comment the significant effect of the NRG1-I isoform on the spinal cord neuroinflammatory response. NRG1-ErbB signaling has been associated with microglial chemotaxis in vitro and in vivo in the spinal cord dorsal horn after peripheral nerve injury (Calvo et al., 2010, 2011). Indeed, it was proved that treatment with an NRG1 antagonist reduced the microglial reactivity in the SOD1^{G93A} mice through the reduction of ErbB2 phosphorylation (Liu et al., 2018). Furthermore, C-boutons degenerate along the course of ALS and in this process the NRG1/ErbB signal-transduction pathway can act as a chemotactic factor for microglia (Casanovas et al., 2017). On the other hand, treatment with NRG1 attenuated astrogliosis following traumatic spinal cord injury (Alizadeh et al., 2017, 2018). Interestingly, we found that overexpression of NRG1-I in the muscles activated cell survival pathways via PI3K/AKT not only in this tissue, but also in the spinal cord, promoting improved MN survival and attenuation of astrocyte and microglial reactivity. Therefore, while NRG1-I might have a deleterious role upon upregulation in the spinal cord of SOD1^{G93A} mice (Song et al., 2012), its overexpression in the muscle preserves the NMJs and the spinal MNs, and thus it can reduce the central neuroinflammatory response. Based on these results, combination of Nrg1-I expression in the muscle and Nrg1-III in the spinal cord may have a synergistic effect on ALS therapy.

Since ALS pathogenesis is considered to develop in a dying-back process, in which the nerve terminals and NMJ are partially degraded when cell bodies in the spinal cord are still intact, viral-mediated NRG1-I therapy may be a suitable approach to counteract this initial degenerative process in MN diseases. However, further experiments should be performed to elucidate the pathways modulated by NRG1-I overexpression in the skeletal muscle. In this study, we introduced a therapeutic strategy to deliver NRG1-I in most skeletal muscles of the SOD1^{G93A} mice with a single systemic injection. Therefore, this viral-mediated therapy can be considered for the translation to treat ALS patients since it is minimally invasive, only requires a single administration, permits the wide overexpression of the gene of interest skeletal muscles affected in ALS but not in other cell types, and allows a long-term expression even at the end-stage of the disease.

Supplementary data to this article can be found online at https://doi.org/10.1016/j.nbd.2020.104793.

Declaration of Competing Interest

The authors report no conflicts of interest. The authors alone are responsible for the content and writing of the paper.

Acknowledgements

References

Alizadeh, A., Dyck, S.M., Kataria, H., Shahriary, G.M., Nguyen, D.H., Santhosh, K.T., Karimi-Abdolrezaee, S., 2017. Neuregulin-1 positively modulates glial response and improves neurological recovery following traumatic spinal cord injury. Glia 65, 1152–1175.

Alizadeh, A., Santhosh, K.T., Kataria, H., Gounni, A.S., Karimi-Abdolrezaee, S., 2018. Neuregulin-1 elicits a regulatory immune response following traumatic spinal cord injury. J. Neuroinflammation 15, 53.

Andrechek, E.R., Hardy, W.R., Girgis-Gabardo, A.A., Perry, R.L., Butler, R., Graham, F.L., Kahn, R.C., Rudnicki, M.A., Muller, W.J., 2002. ErbB2 is required for muscle spindle and myoblast cell survival. Mol. Cell. Biol. 22, 4714–4722.

Bhinge, A., Namboori, S.C., Zhang, X., VanDongen, A.M.J., Stanton, L.W., 2017. Genetic correction of SOD1 mutant iPSCs reveals ERK and JNK activated AP1 as a driver of neurodegeneration in Amyotrophic Lateral Sclerosis. Stem Cell Rep. 8, 856–869.

Bosco, D.A., Landers, J.E., 2010. Genetic determinants of amyotrophic lateral sclerosis as therapeutic targets. CNS Neurol. Disord. Drug Targets 9, 779–790.

Brites, D., Vaz, A.R., 2014. Microglia centered pathogenesis in ALS: insights in cell interconnectivity. Front. Cell. Neurosci. 8, 117.

Calvo, A.C., Manzano, R., Atencia-Cibreiro, G., Oliván, S., Muñoz, M.J., Zaragoza, P., Cordero-Vázquez, P., Esteban-Pérez, J., García-Redondo, A., Osta, R., 2012. Genetic biomarkers for ALS disease in transgenic SOD1(G93A) mice. PLoS One 7 (3), e32632.

Calvo, M., Zhu, N., Tsantoulas, C., Ma, Z., Grist, J., Loeb, J.A., Bennett, D.L., 2010. Neuregulin-ErbB signaling promotes microglial proliferation and chemotaxis contributing to microgliosis and pain after peripheral nerve injury. J. Neurosci. 30, 5437–5450.

Calvo, M., Zhu, N., Grist, J., Ma, Z., Loeb, J.A., Bennett, D.L., 2011. Following nerve injury neuregulin-1 drives microglial proliferation and neuropathic pain via the MEK/ERK pathway. Glia 59, 554–568.

Casanovas, A., Salvany, S., Lahoz, V., Tarabal, O., Piedrafita, L., Sabater, R., Hernández, S., Calderó, J., Esquerda, J.E., 2017. Neuregulin1-ErbB module in C-Bouton synapses on somatic motor neurons: molecular compartmentation and response to peripheral nerve injury. Sci. Rep. 7, 40155.

Cornblath, D.R., Kuncl, R.W., Mellits, E.D., Quaskey, S.A., Clawson, L., Pestronk, A., Drachman, D.B., 1992. Nerve conduction studies in amyotrophic lateral sclerosis. Muscle Nerve 15, 1111–1115.

Couto, N., Wood, J., Barber, J., 2016. The role of glutathione reductase and related enzymes on cellular redox homoeostasis network. Free Radic. Biol. Med. 95, 27–42.

De Carvalho, M., Swash, M., 2000. Nerve conduction studies in amyotrophic lateral sclerosis. Muscle Nerve 23, 344–352.

De Jesus-Hernandez, M., Mackenzie, I.R., Boeve, B.F., Boxer, A.L., Baker, M., Rutherford, N.J., Nicholson, A.M., et al., 2011. Expanded GGGGCC hexanucleotide repeat in noncoding region of C9ORF72 causes chromosome 9p-linked FTD and ALS. Neuron 72, 245–256.

Esper, R.M., Loeb, J.A., 2004. Rapid axoglial signaling mediated by neuregulin and neurotrophic factors. J. Neurosci. 24, 6218–6227.

Esper, R.M., Pankonin, M.S., Loeb, J.A., 2006. Neuregulins: versatile growth and differentiation factors in nervous system development and human disease. Brain Res. Rev. 51, 161–175.

Federici, T., Boulis, N.M., 2006. Gene-based treatment of motor neuron diseases. Muscle Nerve 33, 302–323.

Ferraiuolo, L., De Bono, J.P., Heath, P.R., Holden, H., Kasher, P., Channon, K.M., et al., 2009. Transcriptional response of the neuromuscular system to exercise training and potential implications for ALS. J. Neurochem. 109, 1714–1724.

Fischer, L.R., Culver, D.G., Tennant, P., Davis, A.A., Wang, M., Castellano-Sanchez, A., Khan, J., Polak, M.A., Glass, J.D., 2004. Amyotrophic lateral sclerosis is a distal axonopathy: evidence in mice and man. Exp. Neurol. 185, 232–240.

Fledrich, R., Stassart, R.M., Klink, A., Rasch, L.M., Prukop, T., Haag, L., Czesnik, D., Kungl, T., Abdelaal, T.A., Keric, N., Stadelmann, C., Brück, W., Nave, K.A., Sereda, M.W., 2014. Soluble neuregulin-1 modulates disease pathogenesis in rodent models of Charcot-Marie-Tooth disease 1A. Nat. Med. 20, 1055–1061.

Fledrich, R., Akkermann, D., Schütza, V., Abdelaal, T.A., Hermes, D., Schäffner, E., Soto-Bernardini, M.C., Götze, T., Klink, A., Kusch, K., Krueger, M., Kungl, T., Frydrychowicz, C., Möbius, W., Brück, W., Mueller, W.C., Bechmann, I., Sereda, M.W., Schwab, M.H., Nave, K.A., Stassart, R.M., 2019. NRG1 type I dependent autoparacrine stimulation of Schwann cells in onion bulbs of peripheral neuropathies. Nat. Commun. 10 (1), 1467.

Gallart-Palau, X., Tarabal, O., Casanovas, A., Sábado, J., Correa, F.J., Hereu, M., Piedrafita, L., Calderó, J., Esquerda, J.E., 2014. Neuregulin-1 is concentrated in the postsynaptic subsurface cistern of C-bouton inputs to α-motoneurons and altered during motoneuron diseases. FASEB J. 28, 3618–3632.

Graffmo, K.S., Forsberg, K., Bergh, J., Birve, A., Zetterström, P., Andersen, P.M., Marklund, S.L., Brännström, T., 2013. Expression of wild-type human superoxide dismutase-1 in mice causes amyotrophic lateral sclerosis. Hum. Mol. Genet. 22, 51–60.

Gurney, M.E., Pu, H., Chiu, A.Y., Dal Canto, M.C., Polchow, C.Y., Alexander, D.D., Caliendo, J., Hentati, A., Kwon, Y.W., Deng, H.X., 1994. Motor neuron degeneration in mice that express a human cu,Zn superoxide dismutase mutation. Science 264, 1772–1775.

Hayworth, C.R., Moody, S.E., Chodosh, L.A., Krieg, P., Rimer, M., Thompson, W.J., 2006. Induction of neuregulin signaling in mouse muscle is sufficient to mimic responses to denervation. J. Neurosci. 26, 6873–6884.

Hippenmeyer, S., Shneider, N.A., Birchmeier, C., Burden, S.J., Jessell, T.M., Arber, S., 2002. A role for neuregulin1 signaling in muscle spindle differentiation. Neuron 36, 1035–1049.

Issa, A.N., Zhan, W.Z., Sieck, G.C., Mantilla, C.B., 2010. Neuregulin-1 at synapses on phrenic motoneurons. J. Comp. Neurol. 518, 4213–4225.

Kabashi, E., Valdmanis, P.N., Dion, P., Spiegelman, D., McConkey, B.J., Van de Velde, C., Bouchard, J.P., Lacomblez, L., Pochigaeva, K., Salachas, F., Pradat, P.F., Camu, W., Meininger, V., Dupre, N., Rouleau, G.A., 2008. TARDBP mutations in individuals with sporadic and familial amyotrophic lateral sclerosis. Nat. Genet. 40, 572–574.

Kügler, S., 2016. Tissue-specific promoters in the CNS. Methods Mol. Biol. 1382, 81–91.

Lasiene, J., Komine, O., Fujimori-Tonou, N., Powers, B., Endo, F., Watanabe, S., et al., 2016. Neuregulin 1 confers neuroprotection in SOD1-linked amyotrophic lateral sclerosis mice via restoration of C-boutons of spinal motor neurons. Acta Neuropathol. Commun. 4, 15.

Li, B., Zheng, Z., Wei, Y., Wang, M., Peng, J., Kang, T., Huang, X., Xiao, J., Li, Y., Li, Z., 2011. Therapeutic effects of neuregulin-1 in diabetic cardiomyopathy rats. Cardiovasc. Diabetol. 10, 69.

Liu, J., Allender, E., Wang, J., Simpson, E.H., Loeb, J.A., Song, F., 2018. Slowing disease progression in the SOD1 mouse model of ALS by blocking neuregulin-induced microglial activation. Neurobiol. Dis. 111, 118–126.

Loeb, J.A., 2003. Neuregulin: an activity-dependent synaptic modulator at the neuromuscular junction. J. Neurocytol. 32, 649–664.

Loeb, J.A., Khurana, T.S., Robbins, J.T., Yee, A.G., Fischbach, G.D., 1999. Expression patterns of transmembrane and released forms of neuregulin during spinal cord and neuromuscular synapse development. Development 126, 781–791.

Loeb, J.A., Hmadcha, A., Fischbach, G.D., Land, S.J., Zakarian, V.L., 2002. Neuregulin expression at neuromuscular synapses is modulated by synaptic activity and neurotrophic factors. J. Neurosci. 22, 2206–2214.

Lopez-Font, I., Sogorb-Esteve, A., Javier-Torrent, M., Brinkmalm, G., Herrando-Grabulosa, M., García-Lareu, B., Turon-Sans, J., Rojas-García, R., Lleó, A., Saura, C.A., Zetterberg, H., Blennow, K., Bosch, A., Navarro, X., Sáez-Valero, J., 2019. Decreased circulating ErbB4 ectodomain fragments as a read-out of impaired signaling function in amyotrophic lateral sclerosis. Neurobiol. Dis. 124, 428–438.

Mancuso, R., Navarro, X., 2015. Amyotrophic lateral sclerosis: current perspectives from basic research to the clinic. Prog. Neurobiol. 133, 1–26.

Mancuso, R., Santos-Nogueira, E., Osta, R., Navarro, X., 2011. Electrophysiological analysis of a murine model of motoneuron disease. Clin. Neurophysiol. 122, 1660–1670.

Mancuso, R., Martínez-Muriana, A., Leiva, T., Gregorio, D., Ariza, L., Morell, M., Esteban-Pérez, J., García-Redondo, A., Calvo, A.C., Atencia-Cibreiro, G., Corfas, G., Osta, R., Bosch, A., Navarro, X., 2016. Neuregulin-1 promotes functional improvement by enhancing collateral sprouting in SOD1(G93A) ALS mice and after partial muscle denervation. Neurobiol. Dis. 95, 168–178.

Mòdol-Caballero, G., Santos, D., Navarro, X., Herrando-Grabulosa, M., 2018. Neuregulin 1 reduces motoneuron cell death and promotes neurite growth in an *in vitro* model of motoneuron degeneration. Front. Cell. Neurosci. 11, 431.

Mòdol-Caballero, G., García-Lareu, B., Verdés, S., Ariza, L., Sánchez-Brualla, I., Brocard, F., Bosch, A., Navarro, X., Herrando-Grabulosa, M., 2019. Therapeutic role of Neuregulin 1 type III in SOD1-linked amyotrophic lateral sclerosis. *Neurotherapeutics*. https://doi.org/10.1007/s13311-019-00811-7. in press.

Moloney, E.B., de Winter, F., Verhaagen, J., 2014. ALS as a distal axonopathy: molecular mechanisms affecting neuromuscular junction stability in the presymptomatic stages of the disease. Front. Neurosci. 8, 252.

Nave, K.A., Salzer, J.L., 2006. Axonal regulation of myelination by neuregulin 1. Curr. Opin. Neurobiol. 16, 492–500.

Pasinelli, P., Brown, R.H., 2006. Molecular biology of amyotrophic lateral sclerosis: insights from genetics. Nat. Rev. Neurosci. 7, 710–723.

Pfaffl, M.W., 2001. A new mathematical model for relative quantification in real-time RT-PCR. Nucleic Acids Res. 29 (9), e45.

Piedra, J., Ontiveros, M., Miravet, S., Penalva, C., Monfar, M., Chillon, M., 2015. Development of a rapid, robust, and universal picogreen-based method to titer adeno-associated vectors. Gene Ther. Methods 26, 35–42.

Renton, A.E., Majounie, E., Waite, A., Simón-Sánchez, J., Rollinson, S., Gibbs, J.R., Schymick, J.C., et al., 2011. A hexanucleotide repeat expansion in C9ORF72 is the cause of chromosome 9p21-linked ALS-FTD. Neuron 72, 257–268.

Ripps, M.E., Huntley, G.W., Hof, P.R., Morrison, J.H., Gordon, J.W., 1995. Transgenic mice expressing an altered murine superoxide dismutase gene provide an animal model of amyotrophic lateral sclerosis. Proc. Natl. Acad. Sci. U. S. A. 92, 689–693.

Robberecht, W., Philips, T., 2013. The changing scene of amyotrophic lateral sclerosis. Nat. Rev. Neurosci. 14, 248–264.

Rosen, D.R., Siddique, T., Patterson, D., Figlewicz, D.A., Sapp, P., Hentati, A., Donaldson, D., Goto, J., O'Regan, J.P., Deng, H.X., 1993. Mutations in cu/Zn superoxide dismutase gene are associated with familial amyotrophic lateral sclerosis. Nature 364, 362.

Sandrock Jr., A.W., Dryer, S.E., Rosen, K.M., Gozani, S.N., Kramer, R., Theill, L.E., Fischbach, G.D., 1997. Maintenance of acetylcholine receptor number by neuregulins at the neuromuscular junction in vivo. Science 276, 599–603.

Schmidt, N., Akaaboune, M., Gajendran, N., 2011. Martinez-Pena y Valenzuela I, Wakefield S, Thurnheer R, Brenner HR. Neuregulin/ErbB regulate neuromuscular junction development by phosphorylation of α-dystrobrevin. J. Cell Biol. 195, 1171–1184.

Song, F., Chiang, P., Wang, J., Ravits, J., Loeb, J.A., 2012. Aberrant neuregulin 1 signaling in amyotrophic lateral sclerosis. J. Neuropathol. Exp. Neurol. 71, 104.

Stassart, R.M., Fledrich, R., Velanac, V., Brinkmann, B.G., Schwab, M.H., Meijer, D., Sereda, M.W., Nave, K.A., 2013. A role for Schwann cell-derived neuregulin-1 in remyelination. Nat. Neurosci. 16 (1), 48–54.

Syed, N., Reddy, K., Yang, D.P., Taveggia, C., Salzer, J.L., Maurel, P., Kim, H.A., 2010. Soluble neuregulin-1 has bifunctional, concentration-dependent effects on Schwann cell myelination. J. Neurosci. 30, 6122–6131.

Syroid, D.E., Maycox, P.R., Burrola, P.G., Liu, N., Wen, D., Lee, K.F., Lemke, G., Kilpatrick, T.J., 1996. Cell death in the Schwann cell lineage and its regulation by neuregulin. Proc. Natl. Acad. Sci. U. S. A. 93, 9229–9234.

Takahashi, Y., Fukuda, Y., Yoshimura, J., Toyoda, A., Kurppa, K., Moritoyo, H., et al., 2013. ErbB4 mutations that disrupt the neuregulin-ErbB4 pathway cause amyotrophic lateral sclerosis type 19. Am. J. Hum. Genet. 93, 900–905.

Timolati, F., Ott, D., Pentassuglia, L., Giraud, M.N., Perriard, J.C., Suter, T.M., Zuppinger, C., 2006. Neuregulin-1 beta attenuates doxorubicin-induced alterations of excitation-contraction coupling and reduces oxidative stress in adult rat cardiomyocytes. J. Mol. Cell. Cardiol. 41, 845–854.

Wijesekera, L.C., Leigh, P.N., 2009. Amyotrophic lateral sclerosis. Orphanet J. Rare Dis. 4, 32.

Wiley, H.S., Woolf, M.F., Opresko, L.K., Burke, P.M., Will, B., Morgan, J.R., Lauffenburger, D.A., 1998. Removal of the membrane-anchoring domain of epidermal growth factor leads to intracrine signaling and disruption of mammary epithelial cell organization. J. Cell Biol. 143, 1317–1328.

Wolpowitz, D., Mason, T.B., Dietrich, P., Mendelsohn, M., Talmage, D.A., Role, L.W., 2000. Cysteine-rich domain isoforms of the neuregulin-1 gene are required for maintenance of peripheral synapses. Neuron 25, 79–91.

Yokoseki, A., Shiga, A., Tan, C.F., Tagawa, A., Kaneko, H., Koyama, A., Eguchi, H., Tsujino, A., Ikeuchi, T., Kakita, A., Okamoto, K., Nishizawa, M., Takahashi, H., Onodera, O., 2008. TDP-43 mutation in familial amyotrophic lateral sclerosis. Ann. Neurol. 63, 538–542.

Zanazzi, G., Einheber, S., Westreich, R., Hannocks, M.J., Bedell-Hogan, D., Marchionni, M.A., Salzer, J.L., 2001. Glial growth factor/neuregulin inhibits Schwann cell myelination and induces demyelination. J. Cell Biol. 152 (6), 1289–1299.

Zolotukhin, S., Byrne, B.J., Mason, E., Zolotukhin, I., Potter, M., Chesnut, K., Summerford, C., Samulski, R.J., Muzyczka, N., 1999. Recombinant adeno-associated virus purification using novel methods improves infectious titer and yield. Gene Ther. 6, 973–985.